Cross-Scale Effects in Solar-Wind Turbulence

F. Valentini,[1] P. Veltri,[1] F. Califano,[2] and A. Mangeney[3]
[1]*Dipartimento di Fisica and CNISM, Università della Calabria, 87036 Rende (CS), Italy*
[2]*Dipartimento di Fisica and CNISM, Universitá di Pisa, 56127 Pisa, Italy*
[3]*Observatoire de Paris-Meudon, 92195 Meudon Cedex, France*
(Received 25 March 2008; published 11 July 2008)

The understanding of the small-scale termination of the turbulent energy cascade in collisionless plasmas is nowadays one of the outstanding problems in space physics. In the absence of collisional viscosity, the dynamics at small scales is presumably kinetic in nature; the identification of the physical mechanism which replaces energy dissipation and establishes the link between macroscopic and microscopic scales would open a new scenario in the study of turbulent heating in space plasmas. We present a numerical analysis of kinetic effects along the turbulent energy cascade in solar-wind plasmas which provides an effective unified interpretation of a wide set of spacecraft observations and shows that, simultaneously with an increase in the ion perpendicular temperature, strong bursts of electrostatic activity in the form of ion-acoustic turbulence are produced together with accelerated beams in the ion distribution function.

DOI: 10.1103/PhysRevLett.101.025006 PACS numbers: 94.05.Lk, 52.35.Fp, 94.05.Pt

The problem of understanding which physical processes ''replace'' dissipation at small scales in a collisionless plasma, like solar wind, is of key relevance in space physics. Several solar-wind observations have shown [1–3] that the short-scale termination of the magnetohydrodynamic (MHD) energy spectra is characterized by the occurrence of significant levels of electrostatic activity, consisting mostly of short-wavelength longitudinal ion-acoustic (IA) waves. The maximum intensity of these fluctuations usually occurs in regions where the particle velocity distributions display strong nonthermal features, like temperature anisotropy and generation of accelerated beams [3–5]. Very recently, Araneda *et al.* [6], using kinetic theory and 1D particle in cell (PIC) hybrid simulations, showed that trapping of ions in modes driven by parametric instability of Alfvén-cyclotron waves generates ion distributions that resemble those observed in solar wind. These evidences suggest that kinetic effects presumably drive the collisionless short-scale system dynamics.

The interpretation of the solar-wind phenomenology at typical kinetic scales [4] would be of far-reaching implications and would represent a significant step forward in the study of turbulent ''heating'' in space plasmas. In this perspective, the fast technological development of supercomputers gives nowadays the possibility of using kinetic Eulerian Vlasov codes that solve the Vlasov-Maxwell equations in multidimensional phase space. The use of these ''zero-noise'' codes is crucial since Eulerian algorithms [7,8] allow for the first time the analysis of kinetic effects in the small-scale tail of the turbulent cascade, where the energy level of the fluctuations is typically very low. In this spectral region, Lagrangian PIC algorithms fail due to their intrinsic statistical noise.

In this Letter, we focus on physical situations where MHD turbulence evolves to a state with power predominantly stored in longitudinal wavevector modes (slab turbulence) [9–11]. The comparison of our numerical results with solar-wind observations shows that: (i) Electrostatic turbulence in longitudinal IA waves represents the main physical cross-scale process of energy transport; (ii) In the development of the turbulent spectra, a novel branch of electrostatic kinetic waves is generated as the results of particle trapping; (iii) This electrostatic activity is associated with temperature anisotropy and generation of accelerated beams in the ion distribution.

To describe the evolution of the plasma, we adopt a hybrid model [8], where ion dynamics is described through Vlasov equation. Electrons are treated as a fluid and a generalized Ohm equation, that retains Hall effect and electron inertia terms, is considered. The Faraday equation, Ampere equation (the displacement current is neglected), and an isothermal equation of state for the electron pressure close the system. Quasineutrality is assumed. The above equations are solved through a numerical hybrid-Vlasov code [8] in 4D phase space, 1D in physical space (with periodic boundary conditions), and 3D in velocity space. In the following, times are scaled by the ion-cyclotron frequency $\Omega_{\rm ci}$, velocities by the Alfvén speed $V_A = B_0/\sqrt{4\pi\rho}$ (B_0 being the magnetic field and ρ the mass density), lengths by the ion skin depth $\lambda_i = V_A/\Omega_{\rm ci}$ and masses by the ion mass m_i.

We assumed that at $t = 0$ the plasma has uniform density and is embedded in a background magnetic field $\mathbf{B}_0 = B_0\mathbf{e}_x$, with superposed a set of circularly left-hand polarized Alfvén waves (x is the direction of wave propagation). The form of velocity and magnetic perturbations [$\delta u_y(x)$, $\delta u_z(x)$, $\delta B_y(x)$, and $\delta B_z(x)$] were derived from the linearized two-fluid equations [8]. Only the first three modes in the spectrum of velocity and magnetic perturbations are excited at $t = 0$ with amplitude $\epsilon = 0.5$. No density dis-

turbances are imposed at $t = 0$. As a consequence, the initial Maxwellian ion distribution is $f(x, \mathbf{v}, t = 0) = A(x) \times \exp[-(\mathbf{v} - \delta\mathbf{u})^2/\beta]$, where $\beta = 2v_{\mathrm{ti}}^2/V_A^2$ ($v_{\mathrm{ti}} = \sqrt{T_i/m_i}$ being the ion thermal speed and T_i the ion temperature); $A(x)$ is such that the velocity integral of f gives the equilibrium density $n_0 = 1$. The electron to ion temperature ratio is set $T_e/T_i = 10$ and $\beta = 0.5$. Perpendicular and parallel ion temperatures at $t = 0$ are $T_\perp = T_\parallel = \beta/2 = 0.25$ and $v_{\mathrm{ti}} = 0.5$. The mass ratio is $m_e/m_i = 1/1836$. The length of the physical domain is $L_x \simeq 40.2$ (the fundamental wave number is $k_1 = 2\pi/L_x \simeq 0.156$), while the limits of the velocity domain in each direction are fixed at $v^{\max} = 5v_{\mathrm{ti}}$. We use 2048 gridpoints in physical space, and 51^3 in velocity space and a time step $\Delta t = 10^{-3}$. The simulation is carried up to $t = 200$.

In the early stage of the system evolution, ponderomotive forces give rise to compressive effects, with density fluctuations $|\delta n/n| \simeq 0.07$, and generate a spatial modulation in $|B|^2$. Moreover, nonlinear three-wave coupling produces a direct energy cascade towards higher wave numbers. At wave numbers close to $k_i = \lambda_i^{-1}$, proton cyclotron resonance with left-handed cyclotron waves [12] produces an increase in the perpendicular temperature and a consequent temperature anisotropy in the ion distribution function [13,14]. As shown in Fig. 1, where $T_\perp$ and $T_\parallel$ are plotted versus x at three different times, the perpendicular heating is not spatially homogeneous, due to the modulation in $|B|^2$, and is generally associated with a decrease in parallel temperature. The effect of perpendicular heating and the corresponding parallel cooling in the process of cyclotron absorption of ion-cyclotron waves has been demonstrated long ago by Arunasalam [15] and Busnardo-Neto *et al.* [16].

Figure 2 reports the numerical spectra of particle density ($|n_k|^2$, red line), and magnetic ($|B_k|^2$, black line), kinetic ($|U_k|^2$, purple line) and electric ($|E_k|^2$, blue line) energies, at different times in the simulation. From Fig. 2, one realizes that the energy transfer to small scales, across λ_i, is not driven by a continuous cascade, but for $t > 30$ a well defined group of wave numbers ($10 < k < 100$) are excited; at $t = 200$ the energy spectra look evidently peaked around $k \simeq 30$ and the magnetic energy is sensibly lower than the electric one, meaning that electrostatic activity is observed. Moreover, short-wavelength spikes of large amplitude appear in the parallel electric field E_x. The top plot of Fig. 3 shows E_x as a function of x at $t = 100$; the middle and the bottom plots show the density fluctuations δn and the x-v_x contours of $\hat{f}(x, v_x) = \int f dv_y dv_z$. Local density depressions and phase space holes are generated in correspondence of the regions of highly impulsive behavior of E_x. These vortices, typical signature of particle trapping, propagate in the positive x direction with velocity close to $v_{\mathrm{ti}} = 0.5$ (black dashed line in the figure).

The signature of electrostatic activity has been detected ubiquitous in interplanetary plasmas. The first evidence of significant levels of electric field turbulence in the solar wind is due to Gurnett and Anderson [1], who in 1977 analyzed plasma wave measurements of the solar-orbiting Helios 1 and 2 spacecrafts near 1 AU. Further analyses of these observations [2,3] showed that the typical energy

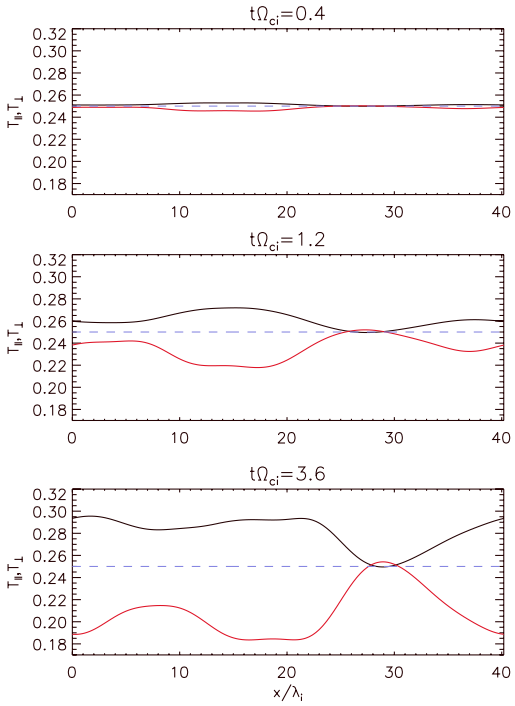

FIG. 1 (color online). Perpendicular (black line) and parallel (red line) temperature versus x at three different times.

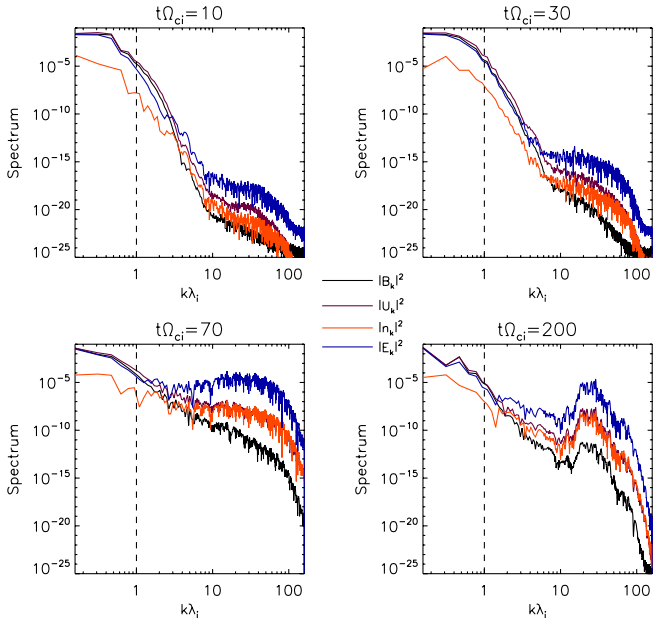

FIG. 2 (color online). Energy spectra at four different times: magnetic energy (black line), electric energy (blue line), kinetic energy (purple line), and density (red line).

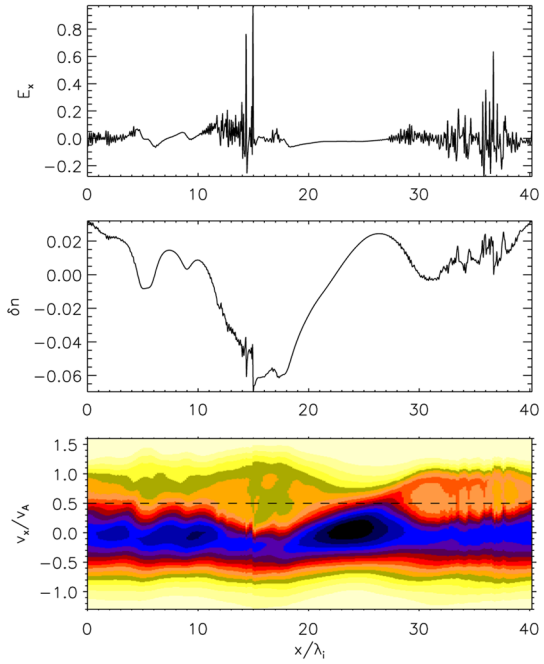

FIG. 3 (color online). (Top plot): parallel electric field (normalized to $E_0 = m_i V_A \Omega_{ci}/e$, e being the electric charge) versus x at $t = 100$. (Middle plot): density fluctuations versus x at $t = 100$. (Bottom plot): x-v_x level lines of the reduced distribution $\hat{f}$ at $t = 100$.

spectra of the parallel electric field appear evidently peaked around 2500 Hz (see Fig. 1 in Ref. [3]), this being the same phenomenology recovered in our simulations. In Ref. [2] this electrostatic turbulence has been identified as short-wavelength IA waves propagating essentially parallel to the ambient field. These fluctuations present a highly impulsive behavior and propagate with frequency below the ion plasma frequency, Doppler-shifted upward by the motion of the solar wind.

To identify the short-wavelength fluctuations observed in the simulation, we considered the k-ω spectrum of the parallel electric energy. This Fourier analysis showed the presence of two acousticlike branches of waves at different phase velocities. The upper branch has a phase velocity $v_\phi \simeq 3.596 v_{ti}$; the numerical dispersion curve for these waves is in extremely good agreement with the dispersion relation of IA waves from Vlasov theory [17], evaluated for wavelengths larger than the Debye length λ_D, $\omega_{IA} = k\sqrt{\beta T_e/2T_i(1 + 3T_i/T_e)}$; this evidence is consistent with the identification by Gurnett *et al.* for the electrostatic fluctuations in solar wind. The unexpected lower branch consists of waves with $v_\phi \simeq 0.925 v_{ti}$. The analysis of the energy spectra for these two branches showed that the IA branch is dominant for $5 < k < 35$, while, for $k > 35$, the energy is predominantly stored in the lower branch with $v_\phi \simeq v_{ti}$.

The nature of these novel electrostatic waves can be investigated by looking for the roots of the electrostatic hybrid-Vlasov dielectric function, in the limit of parallel propagation [17,18]. For Maxwellian velocity distributions, heavily Landau damped roots of the dielectric function are expected at $v_\phi \simeq v_{ti}$, since the wave resonates with the bulk of the distribution [19]. Nevertheless, using a Bernstein-Greene-Kruskal velocity distribution [20], with a plateau in v_x that models particle trapping (see Fig. 3), gives an undamped root at $v_\phi \simeq v_{ti}$. An analogous nonlinear root (electron acoustic waves) has been found with phase velocity close to the electron thermal speed [21,22]. We conclude that the excitation of the lower branch of electrostatic waves recovered in the simulations is driven by kinetic trapping effects. The plateau in the parallel velocity distribution (BGK-like distribution) is created by resonant interaction of ions with parallel propagating ion cyclotron Alfvén waves [23,24].

In 1979 Gurnett *et al.* [3] noted that the intensity of the IA waves in solar wind is large in the low-speed regions, where compressive effects are not negligible, this being the same situation described in our simulations. Moreover, the level of the fluctuations is significantly correlated to the ratio T_e/T_i (the maximum intensity occurs for $T_e/T_i \simeq 10$). Repeating the simulation with several values of T_e/T_i, we noticed that the intensity of the IA peak in Fig. 2 is strongly correlated to T_e/T_i, in agreement with the results discussed by Gurnett. As an example, we found that the energy level of the fluctuations for $T_e/T_i = 1$ is 10 orders of magnitude lower than for $T_e/T_i = 10$. This is not surprising since it is well known from Vlasov theory [17] that for cold electrons IA waves are strongly Landau damped.

From the data in Ref. [3], the typical wavelength of IA waves at 1 AU, corresponding to the frequency $f_{exp} \simeq 2500$ Hz, is $\lambda \simeq 150$ m and the local Debye length is $\lambda_D \simeq 5$ m. For $\lambda_D/\lambda \simeq 0.03$, the Vlasov dispersion relation for IA waves has an acousticlike behavior [17]; therefore, effects of charge separation are not recovered in the data discussed in Ref. [3], this meaning that the solar-wind phenomenology can be successfully reproduced within the hybrid-Vlasov-Maxwell model, despite the quasineutrality assumption. Once the Doppler effect has been eliminated, the angular frequency of the peak of IA waves from space observations at 1 AU is $\omega_{IA}^{exp}/\Omega_{ci} \simeq 1570$, where $\Omega_{ci} \simeq 1$ Hz is the typical ion-cyclotron frequency in the solar wind. The angular frequency for the IA peak from the simulation is $\omega_{IA}^{num} \simeq 52.5$. This value represents the maximum IA frequency allowed by the spatial numerical resolution of our code; indeed, a new simulation performed with $N_x = 4096$ gave rise to a shift of the peak in Fig. 2 towards higher wave numbers.

As discussed in Ref. [3], the generation of double-stream ion distributions [3,5,24,25] has been observed in correspondence with the maximum intensity of electrostatic activity in solar wind. The secondary beam moves along the ambient field with velocity close to the local Alfvén

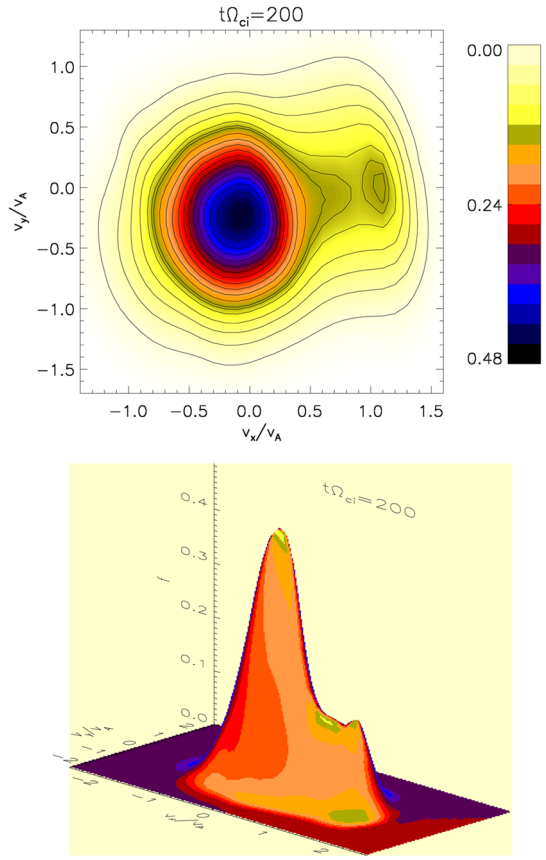

FIG. 4 (color online). Level lines (at the top) and surface plot (at the bottom) of f in the velocity plane v_x-v_y at $t = 200$.

speed. We then analyzed the evolution of the numerical ion distribution in velocity space. As shown in Fig. 3, x-v_x phase space trapping is associated with the short-wavelength activity. The top plot of Fig. 4 displays the v_x-v_y contour lines of the numerical ion distribution at $t = 200$ integrated over v_z and for a given point x_M in the physical domain, x_M being the point where the x-v_x trapping region has maximum velocity width. The bottom plot in the same figure shows a surface plot of the same distribution. A well-resolved proton beam is visible in these two plots, moving along $\mathbf{B}_0$ with velocity $v_b \simeq 1.15V_A$. The phase velocity of the novel kinetic waves recovered in the simulation is located in correspondence of the plateau in between the primary and secondary peaks in Fig. 4, while the phase velocity of IA waves is in the tail of the distribution (outside the depicted velocity domain).

The numerical analysis discussed in the present Letter complements the recent work by Araneda *et al.* [6] discussed above, but especially provides a novel explanation of the bursts of ion-acoustic activity occurring in the solar wind. We conclude that the electrostatic turbulence in space plasmas consists of longitudinal waves with acousticlike dispersion relation and it is associated with the generation of ion-beam distributions. Beside the IA branch, which is in agreement with solar-wind data, the numerical k-ω spectrum indicates the presence of a new branch of kinetic waves propagating at $v_\phi \simeq v_{\mathrm{ti}}$. Unfortunately, the available measurements in space plasmas do not allow a k-ω analysis at typical kinetic scales. In this view, it is desirable that future space missions could provide this crucial information, in order to test the effectiveness of the numerical model predictions.

This work was partially supported by ASI/INAF Grant No. I/015/07/0 "Studi di Esplorazione del Sistema Solare." We are pleased to acknowledge the "Mesocentre SIGAMM" (Observatoire de la Cote d'Azur) where part of the computations were done.

[1] D. A. Gurnett and R. R. Anderson, J. Geophys. Res. **82**, 632 (1977).
[2] D. A. Gurnett and L. A. Frank, J. Geophys. Res. **83**, 58 (1978).
[3] D. A. Gurnett *et al.*, J. Geophys. Res. **84**, 2029 (1979).
[4] R. Bruno and V. Carbone Living Rev. Solar Phys. **2**, 4 (2005) http://www.livingreviews.org/lrsp-2005-4; E. Marsch, Living Rev. Solar Phys. **3**, 1 (2006) http://www.livingreviews.org/lrsp-2006-1.
[5] E. Marsch *et al.*, J. Geophys. Res. **87**, 52 (1982).
[6] J. A. Araneda, E. Marsch, and A. F. Vinas, Phys. Rev. Lett. **100**, 125003 (2008).
[7] A. Mangeney *et al.*, J. Comput. Phys. **179**, 495 (2002).
[8] F. Valentini *et al.*, J. Comput. Phys. **225**, 753 (2007).
[9] M. Dobrowolny, A. Mangeney, and P. Veltri, Astron. Astrophys. **83**, 26 (1980).
[10] W. H. Matthaeus, M. L. Goldstein, and J. H. King, J. Geophys. Res. **91**, 59 (1986).
[11] V. Carbone, F. Malara, and P. Veltri, J. Geophys. Res. **100**, 1763 (1995).
[12] J. V. Hollweg and P. A. Isenberg, J. Geophys. Res. **107**, 1147 (2002).
[13] E. Marsch, X.-Z. Ao, and C.-Y. Tu, J. Geophys. Res. **109**, A04102 (2004).
[14] P. Hellinger and P. Travnichek, Geophys. Res. Lett. **33**, L09 101 (2006).
[15] V. Arunasalam, Phys. Rev. Lett. **37**, 746 (1976).
[16] J. Busnardo-Neto *et al.*, Phys. Rev. Lett. **36**, 28 (1976).
[17] N. A. Krall and A. W. Trivelpiece, *Principles of Plasma Physics* (San Francisco Press, San Francisco, 1986).
[18] F. Valentini (to be published).
[19] L. D. Landau, J. Phys. (Moscow) **10**, 25 (1946).
[20] I. B. Bernstein, J. M. Greene, and M. D. Krukal, Phys. Rev. **108**, 546 (1957).
[21] J. P. Holloway and J. J. Dorning, Phys. Rev. A **44**, 3856 (1991).
[22] F. Valentini, T. M. O'Neil, and D. H. E. Dubin, Phys. Plasmas **13**, 052303 (2006).
[23] C. F. Kennel and F. Engelmann, Phys. Fluids **9**, 2377 (1966).
[24] M. Heuer and E. Marsch, J. Geophys. Res. **112**, A03102 (2007).
[25] C. -Y. Tu, L. -H. Wang, and E. Marsch, J. Geophys. Res. **107**, 1291 (2002).